Supplemental material: "Temperature and coupling dependence of the universal contact intensity for an ultracold Fermi gas"

F. Palestini, A. Perali, P. Pieri, and G. C. Strinati
Dipartimento di Fisica, Università di Camerino, I-62032 Camerino, Italy

Essential equations of the t-matrix approximation above T_c

For the reader convenience, we recall the essential equations of the t-matrix approximation for $T > T_c$ that were originally reported in Ref.[1]:

$$\Sigma(\mathbf{k},\omega_n) = -T\sum_\nu \int \frac{d^3q}{(2\pi)^3}\,\Gamma^{(0)}(\mathbf{q},\Omega_\nu) \times G^{(0)}(\mathbf{q}-\mathbf{k},\Omega_\nu-\omega_n), \quad (1)$$

$$\Gamma^{(0)^{-1}}(\mathbf{q},\Omega_\nu) = -\frac{m}{4\pi a_F} - \int \frac{d^3k}{(2\pi)^3} \times \left[T\sum_n G^{(0)}(\mathbf{k},\omega_n)G^{(0)}(\mathbf{q}-\mathbf{k},\Omega_\nu-\omega_n) - \frac{m}{k^2}\right], \quad (2)$$

$$G^{-1}(\mathbf{k},\omega_n) = G^{(0)^{-1}}(\mathbf{k},\omega_n) - \Sigma(\mathbf{k},\omega_n), \quad (3)$$

$$n = 2T\sum_n e^{i0^+\omega_n}\int \frac{d^3k}{(2\pi)^3}\,G(\mathbf{k},\omega_n). \quad (4)$$

Here, $G^{(0)}(\mathbf{k},\omega_n)$ is the "bare" fermion propagator given by $G^{(0)^{-1}}(\mathbf{k},\omega_n) = i\omega_n - \xi(\mathbf{k})$ [$\xi(\mathbf{k}) = \mathbf{k}^2/(2m) - \mu$ being the free-particle dispersion measured with respect to the chemical potential μ], m is the free-fermion mass, $\omega_n = \pi T(2n+1)$ (n integer) and $\Omega_\nu = 2\pi T\nu$ (ν integer) are, respectively, fermionic and bosonic Matsubara frequencies at temperature T. These equations have been solved numerically according to the procedures described in detail in Ref. [1]. The chemical potential is eliminated in favor of the density n via Eq. (4). The extension of the above set of equations to the superfluid phase was reported in Ref. [2].

Connection between the contact intensity for the whole trap and for a homogeneous system

It is interesting to compare the values of C_t obtained for the whole trap with its approximation obtained from Eq.(2) of the main text, whereby one identifies the shell at $r_{\max}$ corresponding to the maximum of the *radial* weight function $(32/\pi)\,r^2\,[3\pi^2\,n(r)]^{4/3}/k_F^4$, and then takes $C_h(r_{\max})$ therein outside the integral. The result of this procedure at T_c is reported vs the coupling $(k_F a_F)^{-1}$ in Fig. S1(a), where the inset shows an example of the shape of the radial weight function (full line/right scale) and of $C_h(r)$ (dashed line/left scale) at unitarity. The good agreement, which results between the calculation for the trap (full line) and the approximation that selects the contribution of the most important shell (dashed line), shows to what an extent the results of C_t for the whole trap can be used, together with knowledge of the density profiles, to extract the values of C_h for the homogeneous case.

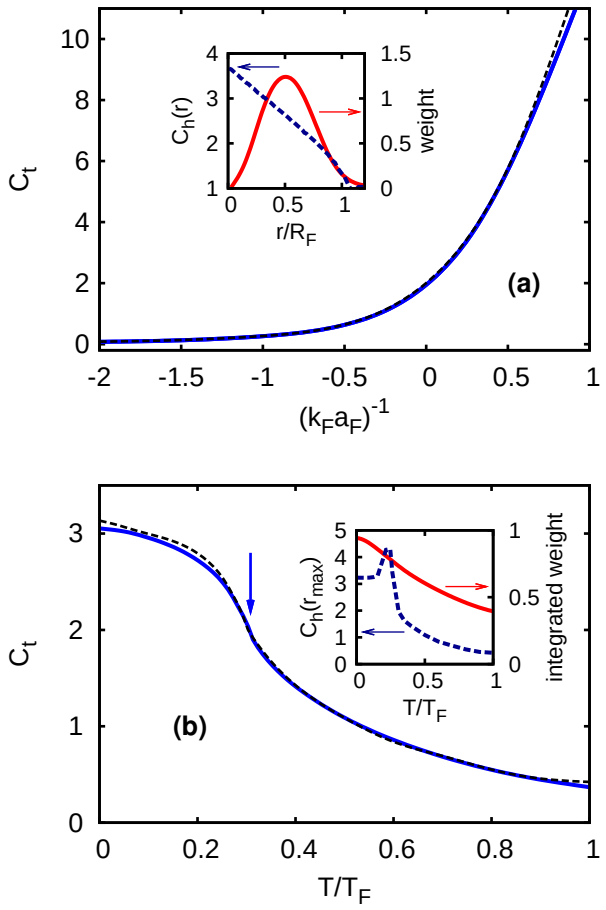

FIG. S1: The contact C_t obtained within the t-matrix approximation for the trapped case, is shown (full line) (a) at T_c vs the coupling $(k_F a_F)^{-1}$, and (b) at unitarity vs T/T_F, and compared with the approximation (dashed line) that relies on the maximum of the radial weight function. [See the text for the meaning of the insets.]

The same procedure can be applied to interpret the temperature dependence of C_t, reported in the inset of Fig. 4 of the main text and reproduced here in Fig. S1(b) for convenience (full line). In particular, it is interesting to understand how the trap averaging washes out the peak about T_c obtained for the homogeneous case (see

Fig. 1(b) of the main text).

To appreciate this effect, we have reported in the inset of Fig. S1(b) the temperature dependence at unitarity of the integral of the radial weight function (full line/right scale) and of $C_h(r_{max})$ (dashed line/left scale) from above to below T_c. While $C_h(r_{max})$ retains the characteristic cusp feature of the homogeneous case (with a maximum at $T = 0.8T_c$), the steady increase of the integrated weight for decreasing temperature more than compensates for the decrease of $C_h(r_{max})$ when $T < 0.8T_c$, thus masking eventually the cusp feature in the integrated quantity.

The same approximate procedure, that resulted in the dashed line of Fig. S1(a), can be applied to reproduce the temperature dependence of C_t at unitarity *above* T_c, because in this case the two functions in the integral of Eq.(2) of the main text have a smooth behavior similar to that shown in the inset of Fig. S1(a). At given T *below* T_c, however, the cusp present in $C_h(r)$ requires us to split it as the sum of a smooth background $C_h^{(b)}(r)$ and of a peaked contribution $C_h^{(p)}(r)$, yielding approximately:

$$C_t \simeq C_h^{(b)}(r_{max}) \frac{32}{\pi} \int_0^\infty dr\, r^2 \frac{[3\pi^2\, n(r)]^{4/3}}{k_F^4} + \frac{32}{\pi} \int_0^\infty dr\, r^2 \frac{[3\pi^2\, n(r)]^{4/3}}{k_F^4} C_h^{(p)}(r)\,. \qquad (5)$$

These approximate results, from above to below T_c, are shown by the dashed line in Fig. S1(b) (to which the second term on the right-hand side of Eq.(5) below T_c gives at most a 15% contribution).

[1] A. Perali, P. Pieri, G. C. Strinati, and C. Castellani, Phys. Rev. B **66**, 024510 (2002).

[2] P. Pieri, L. Pisani, and G. C. Strinati, Phys. Rev. B **70**, 094508 (2004).